J. Biomechanics, 1974, Vol. 7, pp. 67–76. Pergamon Press. Printed in Great Britain

NONLINEAR WAVE PROPAGATION IN VISCOELASTIC TUBES: APPLICATION TO AORTIC RUPTURE*

Y. KIVITY† and R. COLLINS‡

University of California, Los Angeles, California, U.S.A.

Abstract—Recent statistical surveys into the causes of automobile fatalities have shown that traumatic rupture of the aorta followed by immediate exsanguination is responsible for a significant percentage of traffic deaths in the United States. The object of this investigation is to understand a possible mechanism for this failure. A mathematical analysis is presented of the motion of blood in a distensible viscoelastic segment of aorta subjected to a decelerative force field. Calculations of axial wall strain and strain-rate indicate that wave propagation resulting in abrupt shock-like transitions along the aortic wall may well account for the transverse ruptures observed, when compared with the limited amount of rupture data presently available. The analytic method and numerical solution by a two-step Lax–Wendroff differencing scheme are sufficiently general to describe a wide variety of initial and boundary conditions related to blunt impact to the thorax.

1. INTRODUCTION

Blunt impact to the thorax often results in traumatic rupture of the aorta, leading to immediate exsanguination. Current interest in the mechanisms of this failure is great (Roberts and Beckman, 1970), particularly with regard to vehicular fatilities in which passengers are subjected to high levels of deceleration. An estimated 61–83 per cent of all such aortic ruptures occur in automobile collisions. Mechanical forces acting on the wall of the aorta may derive: from the intra-aortic pressure field which changes significantly during impact, from sudden local stretching of the wall at points of relative fixation, or from the effects of nonlinear wave propagation along the aorta. The dominant mechanism(s) responsible for rupture still constitute a subject of considerable controversy in the medical literature (see references). In the next section, a review is presented of the current hypotheses concerning the mechanisms of aortic rupture, followed by a theoretical analysis of the coupled problem of fluid and wall motions for a straight aortic segment subjected to various levels of acceleration.

2. EARLIER INVESTIGATIONS

Rindfleisch (1893) was among the first to observe pathological rupture of the aorta, proposing that its location is in all cases determined by the degree of attachment of the aortic arch and the pulmonary artery. Often a split occurs between the media and adventitia which results in complete isolation of the aorta in an aneurysmic 'sack'. This may then burst outwards, leading to immediate exsanguination. Greendyke (1966) found, in a statistical study, that the common site of rupture was the aortic isthmus, (just distal to the insertion of the ligamentum arteriosum) comprising more than half the cases examined. He affirmed the traditional explanation for the high incidence of ruptures at this location as that due to inertial forces developed during the deceleration. These forces pull on the vessel at its points of fixation, particularly at the arch, where the greatest strain results. Ruptures may also occur in the ascending aorta, proximal to its zone of fixation near the arch. The attachment of the proximal end of the ascending aorta in the heart does not possess the same degree of rigidity, due to the mobility of the heart. Relative mobility of the aorta also exists at the descending thoracic aorta at the diaphragmatic hiatus, and the abdominal aorta, proximal to its bifurcation. The cases of aortic rupture examined by Greendyke in which trauma to the chest was absent caused him to confirm the idea that violent horizontal deceleration alone is adequate to cause rupture. It is noted that rupture was twice as common in occupants who were ejected from the automobile during collision. March and Moore (1957) quoted by Greendyke, estimate that although a vehicle stopping from 30 m.p.h. in a distance of two feet is subjected to a deceleration of 15 g; the passengers, who may stop in inches (relative to the vehicle) may be subjected to 150 g. Head-on collisions may at higher speeds, increase these figures by a factor of 8. In some cases, this effect alone is sufficient to rupture the aorta.

* *Received* 22 *February* 1973.

† On leave of absence from Scientific Department of Ministry of Defense, Israel.

‡ Presently on sabbatical leave at the University of Paris VII, INSERM, 10 Avenue de la Porte d'Aubervilliers, 75019, Paris, France.

Rutherford (1951) reported on four cases of aortic rupture, all occurring in the isthmus region. Since in two of the cases, this constituted the only injury, with no evidence of crushing or flexing of the chest or spine, the mechanism is believed due to a pulling away of the aorta from the well-anchored arch. This produces a tear or rupture immediately distal to the arch. Fidler (1949) observed that spontaneous rupture (due to medio-necrosis) often occurs in the ascending portion of the aorta, and only rarely in the descending portion. Traumatic rupture, on the other hand, may be directed to certain parts of the aorta by virtue of its anatomical attachments. In the age group 23–41, the aorta of adult males is of fairly uniform strength. The great majority of traumatic ruptures occur nonetheless at the aortic insertion of the ligamentum fibrosum. The inherent weakness of the aorta at this point does not appear to be a factor of primary importance.

It is not clear therefore, that rupture is due to high internal pressure in all cases. Certainly in aortic rupture due to falls from great heights, the internal pressure in the aortic arch would be lower than normal if the body strikes the ground on the caudal (tail) end. In this case, it is more reasonable to attribute rupture to mechanical strain.

Shennan (1928) affirmed that the normal aorta can withstand any increased blood pressure due exclusively to a strongly acting left ventricle. Failure of the wall most often occurs by degeneration of various elements of the media.

3. HYPOTHESIS CONCERNING AORTIC RUPTURE

Wilson and Roome (1933) cited by McDonald and Campbell (1945) suggest that injury is most likely at the start of diastole when the aorta is fully distended with blood, whereas Warfield (1933) (quoted by McDonald and Campbell) contends that the important factor is the condition of full inspiration, when the heart is caught between the sternum and the fully inflated lungs. McDonald and Campbell support the theory of Rindfleisch concerning the importance of fixation of the aorta in localizing the rupture area. McKnight *et al.* (1964) (quoted by Pate *et al.*, 1968) state that it is the aortic arch that is mobile, the descending aorta being attached to the left anterolateral border of the vertebral column. They agree with Rindfleisch only in that points of fixation in general determine the zone of concentrated stresses, but differ on the ways in which fixation is produced.

Strassman (1947) presented the findings of 72 cases of aortic rupture examined in New York City during 1936–1942 from a total of approximately 7000 autopsies. The age distribution was from under 10 to over 80 yr of age. In all cases of spontaneous rupture, the tear started within the media. In all cases of traumatic rupture, however, the aorta was completely severed, making it difficult to determine in which layer the tear had begun, although in some survivors the adventitia remained intact. It would appear that in some cases of traumatic rupture, the tear begins in the intima. Strassman found that the majority of traumatic ruptures occurred at the isthmus where the aorta is narrower and relatively fixed by the ligamentum arteriosum. He concluded that the most likely explanation of aortic rupture in a few cases in which there was no evidence of bone fracture or external injury was the sudden increase in intra-arterial pressure caused by the blunt compression of the aorta against the vertebral column.

Gable and Townsend (1963) found in a study of 459 cases of fatal injuries of the cardiovascular system resulting from accelerative forces, that the aorta and its branches were the most commonly involved of all the major blood vessels. In fact, the aorta is far more susceptible to injury than are the other major blood vessels. They also affirmed the importance of accelerative force in causing cardiovascular injury but were not able to choose definitively between that and the hypothesis of Rindfleisch (rupture due to intravascular pressure). They noted, however, the remarkable concurrence of findings among many researchers that the highest incidence of injury was just distal to the left subclavian artery; i.e. in the region of the ductus, for cases of isolated aortic ruptures. When heart lesions were present, the incidence of rupture above the aortic valve was double that of the ductus region.

Taylor (1962) has demonstrated on pigs that, during acceleration, an emptying of the distal half of the thoracic aorta occurs with engorgement of the upper half and of the arch. This retrograde flow may increase the pressure sufficiently in the region of the arch to cause rupture here.

Lundevall (1964) has suggested that geometric distortion of the aorta in the sagittal plane during deceleration will cause local longitudinal stretching of the aortic wall at the two points of fixation; i.e. at the base of the heart and at the isthmus.

In traffic accidents, the contact of the lower portion of the steering wheel with the abdomen may push the abdominal viscera upwards. The left lung may press upward against the aortic arch, causing increased bending or even kinking of the arch. A transverse rupture results near the isthmus. In addition, the cervical vessels may stretch during head motion, exerting longitudinal forces on the aortic wall. Internal pressure in the aortic arch may rise suddenly, due both to compression of the heart and forward inertial motion of the blood already in the arch.

The equations of motion for the blood and the aortic wall are formulated in the next section. Their numerical solution in the following section then allows one to evaluate the dependence of wall stresses (in terms of strain and strain rate) on the magnitude of acceleration, wall viscoelasticity, and on the geometry of the aortic segment as characterized by its length, taper, and wall thickness. Calculations are made up to acceleration levels of 150 g in order to evaluate some of the current hypotheses described above.

4. NONLINEAR WAVE PROPAGATION IN THE AORTA

4.1 *Mathematical formulation*

One adopts a quasi one-dimensional model (Olsen and Shapiro, 1967; Rudinger, 1970; Lambert, 1958) for the flow of an incompressible fluid in a distensible tube, based on the assumptions that (a) the wave length is long compared to the tube diameter and (b) that the tube is constrained from longitudinal motion. The wall material is assumed to be viscoelastic, but fluid viscosity is neglected since its effect on the flow in the larger arteries is insignificant. Under these conditions the governing equations of motion are

$$\frac{\partial A}{\partial t} + \frac{\partial}{\partial x}(Au) = 0 \text{ (Continuity)} \tag{1}$$

$$\frac{\partial u}{\partial t} + u\frac{\partial u}{\partial x} + \frac{1}{\rho}\frac{\partial p}{\partial x} = G \text{ (Momentum)}. \tag{2}$$

Here t denotes the time and x the distance along the axis of the tube (see Fig. 1), u the fluid velocity (averaged over the cross-section), A the cross-sectional area, p the pressure, ρ the constant density of the fluid and G the body force resulting from acceleration or a gravitational field.

To these equations one must add a relation between pressure and cross-sectional area. If the pressure p is assumed to be a function of A alone, the resulting differential equations are hyperbolic, admitting discontinuous solutions (shock waves). In the present study for a viscoelastic tube, the pressure depends also on the time rate of change of the cross-sectional area, $\eta = \partial A/\partial t$. The pressure-area relation is expressed as

$$p = f(A) + g(A, \eta); \quad \eta = \frac{\partial A}{\partial t} \tag{3}$$

where the function $f(A)$ corresponds to static loading, and the term $g(A, \eta)$ accounts for the viscoelastic properties of the wall. g Is a monotonically increasing function of η, with $(A, 0) = 0$.

With the relation (3) the differential equations take on a parabolic character, and mathematical discontinuities are not admissible. Shock-like transitions may develop, however, in the form of very steep (but continuous) wave fronts.

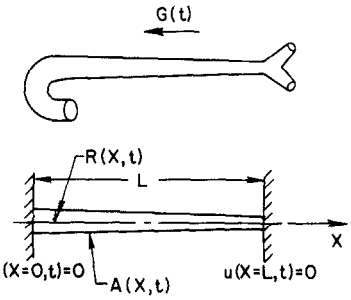

Fig. 1. Geometric idealization of aorta in an accelerative force field.

To complete the mathematical description one must specify initial and boundary conditions. For the problem considered in this study these are:

Initial conditions

$$u(x, 0) = 0 \tag{4}$$

$$A(x, 0) = A_0(x) \tag{5}$$

$$\eta(x, 0) = \frac{\partial A}{\partial t}(x, 0) = 0. \tag{6}$$

The pressure relation employed here (see next section, equation 24) implies, for these initial conditions, that $p(x, 0) = 0$ referred to some base pressure.

Boundary conditions

$$u(0, t) = 0$$
$$u(L, t) = 0. \tag{7a}$$

The physical reasons underlying the choice of these conditions are described in Section 6.

One $A(x, t)$ is determined in the above problem, the axial strain and strain-rate follow directly. The inside tube radius $R(x, t) = \{A(x, t)/\pi\}^{\frac{1}{2}}$ whence

$$\epsilon_a = \left\{1 + \left(\frac{dR}{dx}\right)^2\right\}^{1/2} - 1 \tag{7b}$$

and

$$\dot{\epsilon}_a = \partial \epsilon_a / \partial t.$$

The initial value of the axial strain has been neglected in the above expression, since it is negligibly small. In fact, the intial radius of the tapered tube is given as $R = R_i e^{-0.0225x}$, from which one may estimate $\epsilon_a(t = 0) = 2.5 \times 10^{-4}$, a value too small to appear in Figs. 4–6.

4.2 *Numerical solution*

Equation (4.2) may be written as

$$\frac{\partial u}{\partial t} + \frac{\partial}{\partial x}\left(\frac{u^2}{2} + \frac{p}{\rho} + \phi\right) = 0 \tag{8}$$

where

$$\frac{\partial \phi}{\partial x} = -G. \tag{9}$$

The set of equations (1 and 9) is in conservation form, and therefore the numerical solution may be based on the Lax–Wendroff difference scheme (Richtmyer and Morton, 1967).

Without performing a rigorous stability analysis of the set of equations (1, 3 and 8), it appears sufficient to impose two stability criteria relating to both the hyperbolic and parabolic aspects of the equations. The time interval for integration is determined at each step as the more restrictive of the two, and has been found satisfactory in all cases computed.

The hyperbolic stability criterion may be expressed as

$$\Delta t = \frac{\lambda \Delta x}{(|u| + c)} \max \tag{10}$$

where c is the speed of sound based on the pressure-area relation for static loading

$$c^2 = \frac{A}{\rho} \frac{\mathrm{d}f(A)}{\mathrm{d}A} \tag{11}$$

and λ is a constant <1. In our calculations λ was taken equal to $\frac{1}{2}$. This condition implies that the time step should not be larger than one-half the transit time for a wave propagating through a particular calculational cell.

The parabolic stability criterion is based upon the following deviation. First one defines a new variable

$$F = Au \tag{12}$$

and writes the differential equation in terms of A and F. The continuity equation becomes

$$A_t + F_x = 0. \tag{13}$$

The momentum equation is multiplied by A and is added to u times the continuity equation (13). This gives

$$F_t + \left(\frac{F^2}{A}\right)_x + c^2(A)A_x + \frac{A}{\rho}\left[\frac{\partial g}{\partial A} A_x + \frac{\partial g}{\partial \eta} \eta_x\right] = 0 \tag{14}$$

where the constitutive relation (3) has been used to eliminate p. The quantity η_x may be expressed in terms of F using equation (13), as

$$\eta_x = \frac{\partial^2 A}{\partial x \partial t} = -\frac{\partial^2 F}{\partial x^2}$$

so that equation (14) becomes:

$$F_t - \left(\frac{A \partial g}{\rho \partial \eta}\right) F_{xx} + \left(\frac{F^2}{A}\right)_x + \left(c^2(A) + \frac{A}{\rho} \frac{\partial g}{\partial A}\right) A_x = 0. \tag{15}$$

The form of this equation is obviously similar to that of the heat equation, if one disregards the last two terms. The parabolic stability criterion is given by (Richtmyer and Morton, 1967, pp. 195, 205)

$$\frac{\sigma \Delta t}{\Delta x^2} < \frac{1}{2} \tag{16}$$

where

$$\sigma = \frac{A}{\rho} \frac{\partial g(A, \eta)}{\partial \eta}. \tag{17}$$

Alternatively, it is possible to formulate the flow problem in terms of a single function ψ, defined from equation (13) by

$$\psi_x = A, \quad \psi_t = -F. \tag{18}$$

The resulting third-order differential equation for ψ follows from equations (15 and 18). Although this form was not used here, it may be of interest in devising other computational schemes.

The governing differential equations (1 and 8) are written in difference form, according to the two-step Lax–Wendroff scheme, which is known to possess useful properties of stability:

Step I

$$A_{j+1/2}^{n+1/2} = \frac{1}{2}(A_{j+1}^n + A_j^n) - \frac{1}{2} \frac{\Delta t^n}{\Delta x}[(Au)_{j+1}^n - (Au)_j^n]$$
$$u_{j+1/2}^{n+1/2} = \frac{1}{2}(u_{j+1}^n + u_j^n) - \frac{1}{2} \frac{\Delta t^n}{\Delta x}(q_{j+1}^n - q_j^n) \tag{19}$$

where

$q = \left(\frac{u^2}{2}\right) + \frac{p}{\rho} + \phi$ and q_j^n is defined by

$$q_j^n = \left(\frac{u^2}{2}\right)_j^n + \phi(x_j, t^n) + \frac{1}{\rho}[f(A_j^n) + g(A_j^n, \eta_j^n)]$$

and

$$\eta_j^n = (A_j^n - A_j^{n-1})/\Delta t.$$

Step II

$$A_j^{n+1} = A_j^n - \frac{\Delta t^n}{\Delta x}[(Au)_{j+1/2}^{n+1/2} - (Au)_{j-1/2}^{n+1/2}]$$
$$u_j^{n+1} = u_j^n - \frac{\Delta t^n}{\Delta x}(q_{j+1/2}^{n+1/2} - q_{j-1/2}^{n+1/2}) \tag{20}$$

where

$$q_{j+1/2}^{n+1/2} = \left(\frac{u^2}{2}\right)_{j+1/2}^{n+1/2} + \phi\left(\frac{x_j + x_{j+1}}{2}, t^n + \frac{1}{2}\Delta t^n\right)$$

$$+ \frac{1}{\rho}[f(A_{j+1/2}^{n+1/2}) + g(A_{j+1/2}^{n+1/2}, \eta_{j+1/2}^{n+1/2})]$$

and

$$\eta_{j+1/2}^{n+1/2} = [A_{j\,q1/2}^{n+1/2} - \tfrac{1}{2}(A_{j+1}^n + A_j^n)]/(\tfrac{1}{2}\Delta t'').$$

The j subscripts indicate intervals in distance x along the tube, while the n superscripts denote the time interval.

The initial and bondary conditions (4–7) are simply states as:

$$\left.\begin{aligned} u_j^0 &= 0 \\ A_j^0 &= A_0(x_j); x_j = (j-1)\Delta x \\ \eta_j^0 &= 0 \\ u_1^n &= 0 \\ u_j^n &= 0 \\ u_{jm}^n &= 0. \end{aligned}\right\} \quad (21)$$

Where the indices $j = 1$ and $j = jm$ denote the ends $x = 0$ and $x = L$, respectively. At the end points, Step II must be modified as follows:

$$\left.\begin{aligned} u_1^{n+1} &= 0 \\ A_1^{n+1} &= A_1^n - \frac{\Delta t^n}{\frac{1}{2}\Delta x}(Au)_{1/2}^{n+1/2} \\ u_{jm}^{n+1} &= 0 \\ A_{jm}^{n+1} &= A_{jm}^n + \frac{\Delta t^n}{\frac{1}{2}\Delta x}(Au)_{jm-1/2}^{n+1/2} \end{aligned}\right\} \quad (22)$$

The system is integrated in a step-wise marching procedure in time. The initial values of equations (21) are used to evaluate the right-hand sides of equation (19), from which one obtains the new values of A and u at the next half time step for each position x. These, in turn, are used to evaluate the right-hand sides of (20), which then yield the values of A and u advanced to the full time step. Relations (22) are used to determine u, A at the proximal and distal ends of the aorta at each time step. One then returns to the first step and continues in time.

5. CONSTITUTIVE MODEL FOR AORTA UNDER DYNAMIC LOADING

Generally, soft tissue and muscles behave as nonlinear viscous materials whose stiffness increases with increasing strain-rate. For the dynamic loading rates associated with thoracic impact, it appears that the influence of strain-rate on resulting tissue stresses is of paramount importance. Measurements of Collins and Hu (1972a) for fresh aortic tissue have resulted in a dynamic stress–strain relation, valid for strain-rates up to 3·5 sec^{-1} in the form

$$\sigma = 0{\cdot}28 \times 10^6 (1 + 0{\cdot}644\dot{\epsilon})(e^{1{\cdot}2\epsilon} - 1)\,\text{dyn/cm}^2 \quad (23)$$

where the strain-rate $\dot{\epsilon}$ is measured in inverse seconds.

For an isotropic material, one may deduce from the above expression a relation between the transmural pressure $(p - p_0)$ and the intraluminal cross-sectional area A.

The true strain is defined by

$$\epsilon \equiv \ln\frac{L}{L_0} = \tfrac{1}{2}\ln\frac{A}{A_0}$$

where L is the extended length of an elemental segment, and L_0 its original length.

From the force balance on a thin cylindrical element of thickness h, the transmural pressure is given by

$$p - p_0 = \frac{\sigma h}{R}$$

where R is the radius of curvature of the element. Using a Poisson ratio of one-half (isovolumetric deformation) which is typical of soft biological tissue

$$hR = H_0 R_0$$

whence

$$p - p_0 = \Delta p_2 = f(A) + g(A, \dot{A}) \quad (24)$$

where

$$f(A) = \frac{\rho c_0}{n}\left[\left(\frac{A}{A_0}\right)^{n-1} - \frac{A_0}{A}\right]; n = 6$$

and

$$g(A, \dot{A}) = B|f(A)|\frac{\dot{A}}{A}; B = 0{\cdot}322\ \text{sec}.$$

In the above expression for $f(A)$, the multiplying factor has been determined from the definition for sound speed in a distensible tube

$$C_0^2 = \left(\frac{A}{\rho}\frac{df}{dA}\right)_{A=A_0}$$

where ρ is the constant fluid density.

The absolute modulus appearing in the function g has been added to deal with the range of wall deformation in which $A/A_0 < 1$, so that the condition of increasing stiffness at increasing strain-rate ($g > 0$ for $\dot{A} > 0$) may be maintained even if the aorta should constrict below its reference cross-sectional area A. This

'reflection' of the stress–strain curve for $A/A_0 < 1$ appears reasonable in the absence of other experimental data. The variation of sound speed c_0 and reference cross-sectional area A_0 with distance x along the axis of the vessel may be given in the form

$$c_0(x) = c_i(1 + \beta_1 x) \tag{25}$$

$$A_0(x) = A_i \exp(-\beta_2 x) \tag{26}$$

where the parameters have been estimated by Anliker *et al.* (1971) as $c_i = 300$ cm/sec, $\beta_1 = 0{\cdot}02$/cm, $\beta_2 = 0{\cdot}045$/cm for dogs aortae, and $A_i = \pi$ cm^2 in experiments of Hanson (1970).

However, for large decelerative fields, the strain-rate may well exceed the maximum value of 3·5 sec^{-1} of the experiments of Collins and Hu by 1–½ decades ($10^{1{\cdot}5}$). To the knowledge of the authors, no data are available in that range of strain-rate which could serve to guide the extrapolation of the test results. One must then turn to other sources of data. It is known that an equivalence can be established between tensile tests at high strain rates and those at low temperatures.

When a viscoelastic material is stretched at a particular rate, two competing process act to determine the stress–time response: (a) the progressive deformation of internal bonds, which tends to increase the stress and (b) a continuous relaxation which alleviates the stress. If the material is strained slowly (and at high temperatures) the relaxation process is very rapid relative to the time scale of the deformation, and a continuous equilibrium is maintained. However, the departure form equilibrium becomes progressively greater as the test temperature is decreased, or the extension rate is increased. At high strain rates or at low temperatures, the material cannot accommodate rapidly enough to reach a continuous state of equilibrium. The effective stiffness of the material increases as one departs from the equilibrium state by either of these means. The availability of stress–strain data at low temperatures and low strain rates (e.g. Polmanteer *et al.*, 1952) tempts one to deduce from them the corresponding stress–strain response at high strain rates and normal ambient temperatures.

A method for doing this has been described by Macgregor and Fisher (1946) and summarized in the book by McClintock and Argon (1966). The result may be stated simply: the stress corresponding to a test at an arbitrary strain-rate $\dot{\epsilon}$ and an arbitrary temperature T will be the same as for a test at the strain-rate $\dot{\epsilon}_0$ and temperature $T(1 - k \log_e \dot{\epsilon}/\dot{\epsilon}_0)$, where k is a constant. That is, if the stress corresponding to strain-rate $\dot{\epsilon}$ and temperature T is plotted against the modified temperature abscissa $T(1 - k \log_e \dot{\epsilon}/\dot{\epsilon}_0)$, the resultant curve will coincide with the stress versus temperature curve for strain-rate $\dot{\epsilon}_0$. Thus, stress–strain data at low temperature may be interpreted as data at high strain-rates. However, even here, published experimental data presently available are not grouped suitably to carry out such a conversion.

A more promising approach was found in the work of Smith (1962) who measured stress–relaxation data at large strains for certain elastomers. He showed that the time and strain dependence are separable, so that a constant-strain-rate modulus $E(t)$ may be introduced in the form

$$E(t) = \frac{H(\epsilon)\,\sigma(\epsilon, t)}{\epsilon}$$

and the time t required to reach the selected strain at each strain-rate is obtained as $\epsilon/\dot{\epsilon}$. The experimentally determined relation of Collins and Hu, is quite fortuitously of the same functional form, for large ϵ, with

$$E(t) = \frac{1}{t} = \frac{\dot{\epsilon}}{\epsilon},\ H(\epsilon) = \frac{1}{0{\cdot}18(e^{1{\cdot}2\epsilon} - 1)}. \tag{24}$$

Now we wish to extrapolate the measured relation through 1–½ decades ($10^{1{\cdot}5}$) of $\dot{\epsilon}$ up to $\sim 100\,\text{sec}^{-1}$. Then according to Smith, the function $H(\epsilon)$ is independent of time, and hence strain-rate divided by strain, provided one remains within the time span represented by the experimental data. That is, the function $H(\epsilon)$ should not change its form, even at higher strain-rates. The relative invariance of $H(\epsilon)$ with time has been observed for a number of amorphous elastomers (e.g. styrene butadiene rubber vulcanizate and NBS polyisobutylene) where $H(\epsilon)$ depends only on strain over about 3 decades of time for temperatures between −42·8 and 93·3°C.

Since the measured stress–strain relation of Collins and Hu (1972), which was based purely on experimental results, just happens to possess the same functional form of Smith, it is quite justifiable to broaden its validity directly to higher strain-rates by virtue of the above described properties of Smith's function $H(\epsilon)$. The experimentally determined relation is therefore used in its original form in the numerical solution of the general equations of motion.

6. RESULTS AND DISCUSSION

A number of examples were computed with a view to illustrating the dependence of strain and strain-rate (and hence wall stress) to: (a) the magnitude of the viscoelasticity of the wall, (b) the amplitude and duration of the acceleration history, and (c) the length and taper of the tube.

The geometry of the aorta and its idealization into a straight tapered segment is shown in Fig. 1. The aorta is subjected to an accelerative field directed from

the thoracic aorta towards the aortic arch, corresponding to the type of decelerations measured by Hanson (1970) in which a series of anesthetized beagle dogs was exposed to head-first impact ($-G_z$) over a range of 5–60G. Such accelerations occur in humans during, for example, a head-on vehicular collision in which the passenger is pitched forward over the steering wheel, his back becoming horizontal, and parallel to the direction of motion of the vehicle. The abrupt deceleration caused forward motion of the blood in the descending aorta towards the aortic arch.

A typical acceleration-time history is depicted in Fig. 8, the shape of which may be very closely approximated by two sine curves of equal amplitude (at time t_m) but differing wave length, with total duration $t = T$.

In equation (9) on may express

$$\frac{\partial \varphi}{\partial x} = -G(t) = -G_m \begin{cases} \sin \dfrac{\pi}{2} \dfrac{t}{t_m} & \text{for} \quad t \leqslant t_m \\ \cos \dfrac{\pi}{2} \dfrac{t - t_m}{T - t_m} & \text{for} \quad t_m < t \leqslant T \end{cases}$$

according to the measurements in Hanson's experiment 4F. The parameters T, t_m and G_m are approximated by

$$T = 49{\cdot}5 \text{ ms}, \quad t_m = 17 \text{ ms},$$

$$G_m = 50 \text{ g} = 49{,}050 \text{ cm/sec}^2.$$

Hanson gives measurements of the acceleration, intra-aortic pressure, and intrapleural pressure as a function of time. From the latter two, one may calculate the transmural pressure across the aortic wall. Measurements of intrapleural pressure are particularly susceptible to error as a result of stress concentrations which may develop around the embedded pressure transducer (see Collins *et al.*, 1972b). However, knowledge of the transmural pressures is essential for comparison with the analysis of the stresses which develop in the aortic wall. The results of the impact experiments of Kroell *et al.* (1971) are therefore of very limited use in this respect, since intrapleural pressures were not recorded in their work.

The physical behavior of a fluid-filled viscoelastic tube is portrayed in Figs. 2–7, in which Hanson's experiment with dog No. 4 and acceleration pattern F (see his Fig. 6) was computed using his initial data, as a means of checking the present analysis. For this purpose, it was found that the value of $B = 0{\cdot}08$ sec was more appropriate for dog's aortae, as will be described shortly, than the value of $B = 0{\cdot}322$ sec (equation 24) as implied in the Collins and Hu experiments with pigs

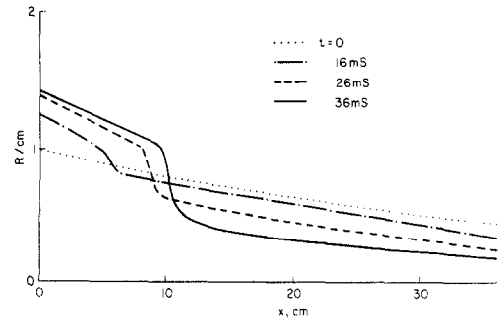

Fig. 2. Calculated variation of inside radius of aorta for Hanson's experiment 4-F, with $B = 0{\cdot}08$ sec.

and human aortae. The initial taper of the aorta is plotted in Fig. 2 for time $t = 0$. For later times (with $B = 0{\cdot}08$ sec), a rapid change in cross-section indicates the formation of a shock wave reflecting from the fixed end $x = 0$ and travelling to the right in the counter-direction to the blood flow. This steepening of the slope of the aortic wall leads to high axial stresses and strains which may eventually culminate in transverse rupture of the aorta. The corresponding fluid velocities (directed to the left) are shown in Fig. 3. Their position of steepening corresponds to that of the wall steepening of Fig. 2, and appears to confirm the existence of a 'shock' front in the flow. Behind the front, the flow velocity reaches a plateau at early times, and is gradually altered as the effect of the boundary condition at $x = L$ transmits its influence towards the aortic root.

The experiments of Hanson do not reveal the correct boundary condition at $x = L$; however, it appears plausible to take $u(L, t) = 0$ since the vascular bed cannot respond rapidly to a 50 msec event. Furthermore, such bondary condition corresponds closely to the classic steering wheel impact (Beck, 1935), in which the steering wheel of the colliding vehicle penetrates into the lower abdomen of the driver, as he is subjected to a head-first deceleration. It is observed in Fig. 3 that the peak velocity decreases after 26 ms. The distributions of axial wall strain and strain-rate along the

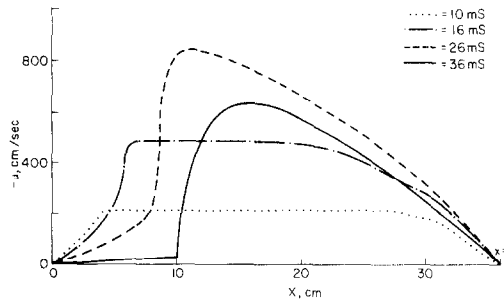

Fig. 3. Calculated variation of blood velocity for Hanson's experiment 4-F, with $B = 0{\cdot}08$ sec.

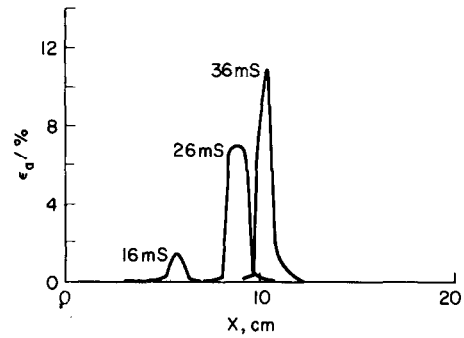

Fig. 4. Calculated variation of axial wall strain for Hanson's experiment 4-*F*, with $B = 0{\cdot}08$ sec.

length x of the tube are plotted in Figs. 4 and 5, revealing peaks which again correspond to the passage of the shock. Axial strain-rates are seen to diminish after 26 msec, as did the peak fluid velocity. Figures 6 and 7 show the time variation of the maximum values of strain and strain-rate over the tube length. It is to be noted that the curve of Fig. 7 is not simply the slope of the curve of Fig. 6, since the maxima of ϵ_a and $\dot{\epsilon}_a$ do not necessarily correspond to the same x-positions at a given time t. The maximum value of $\dot{\epsilon}$ occurs at about 27 msec, preceding the maximum strain by about 5 msec.

Calculations of the transmural pressure at $x = 0$ as a function of time (Fig. 8) show a definite sensitivity to the value of the viscoelasticity B. For $B = 0{\cdot}08$, the amplitude of the pressure variation, and its phase lag relative to the acceleration curve, closely matches the experimental results of Hanson for dog No. 4-*F*, once the origins have been made to coincide. Computations with this value of B also lead to reasonable agreement

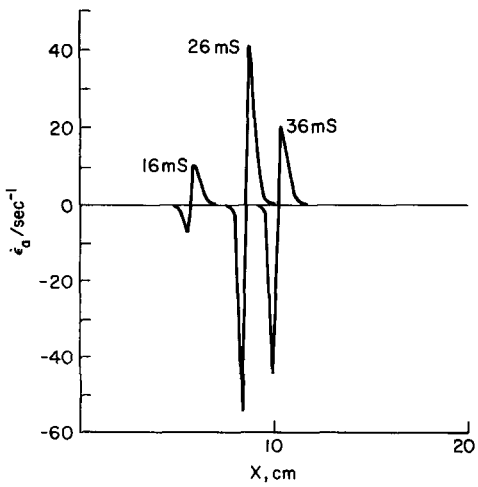

Fig. 5. Calculated variation of axial strain-rate for Hanson's experiment 4-*F*, with $B = 0{\cdot}03$ sec.

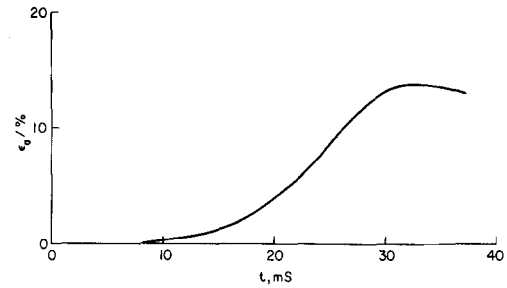

Fig. 6. Variation of maximum wall strain with time for Hanson's experiment 4-*F*, with $B = 0{\cdot}08$ sec.

with the one other Hanson experiment calculated, run 4-*C*, and appear to lend adequate credence to the predictive ability of the present analysis and numerical scheme. Again, note is taken of the inherent inaccuracies associated with the difficult measurements of intrapleural pressures (Collins *et al.*, 1972b).

The transmural pressure is shown (Fig. 9) to be quite sensitive to even very slight tapering of the aorta; it is clear that the aortic taper must always be reported if associated experimental results are to be interpreted meaningfully.

The maximum values of the strain and strain-rate over both x and t are shown in the semi-logarithmic plot of Fig. 10 to be much more sensitive to variations in viscoelasticity B than is the transmural pressure. In fact it would appear very worthwhile to formulate an experimental procedure for determining the unknown visoelastic properties of materials on the basis of shock experiments in which axial strains and strain-rates are recorded. As the viscoelasticity decreases, the shock steepness increases, with concomitant increases in the local strain and strain-rate.

The remaining calculations were carried out with a value of $B = 0{\cdot}12$ s instead of $B = 0{\cdot}08$ s for the sake of economy, as the computational time, which increases markedly for decreasing B, doubles between these two values. The results for $B = 0{\cdot}12$ s are equally indicative of the sensitivity of ϵ_a and $\dot{\epsilon}_a$ to changes in the acceleration.

The maximum strain and strain-rate depends very critically upon the level and duration of the acceleration. For a constant duration 49·5 msec, which is

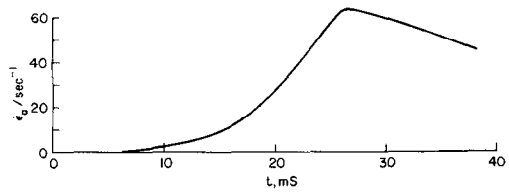

Fig. 7. Variation of maximum strain rate for Hanson's experiment 4-*F*, with $B = 0{\cdot}08$ sec.

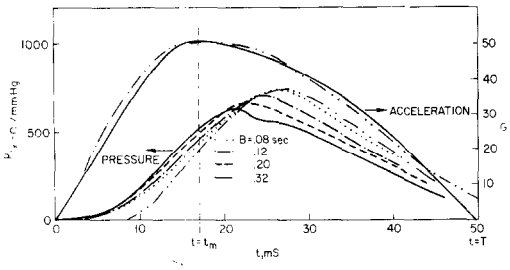

Fig. 8. Accelerations and intra-aortic pressures: (i) Acceleration: - · · — measured by Hanson (experiment 4-F); — — as approximated here by function $G(t)$; (ii) Calculated pressures for various B, compared with —. .— curve measured by Hanson (Experiment 4-F).

quite typical of automobile acidents in which aortic rupture occurs, Fig. 11 depicts a smooth monotonic increase of ϵ_a and $\dot{\epsilon}_a$ with acceleration within the range of 25–100G. It is clear that the total kinetic energy expended in the impact also increases with G if the duration is held constant. In Fig. 12, the variation of ϵ_a and $\dot{\epsilon}_a$ with acceleration has been calculated for constant initial impact velocity $u_I = \int_0^T G dt \simeq 15{\cdot}7$ m/s and appears to be almost linear. In this case, higher levels of accelerations are applied over shorter periods so that the kinetic energy of impact remains constant. These results are useful in the design of vehicles and restraint systems to protect passengers in a collision from a specified initial velocity. Representative data on aortic rupture strengths, when available, will permit one to set definite tolerance levels on impact velocities and acceleration levels.

7. CONCLUSIONS

This investigation provides the first detailed theoretical and numerical treatment of the dynamic response of an aorta to strong decelerative force fields yet known to the authors, and bears directly on the phenomenon of traumatic rupture of the aorta.

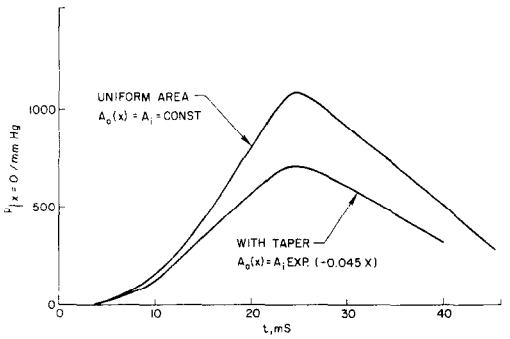

Fig. 9 Influence of wall taper on intra-aortic pressure for Hanson's experiment 4-F, with $B = 0{\cdot}12$ sec.

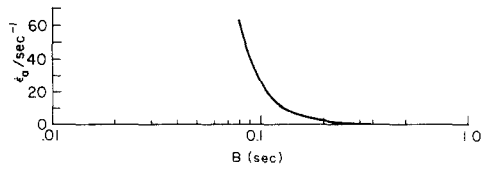

Fig. 10a. Variation of axial strain-rate with viscoelasticity for Hanson's experiment 4-F.

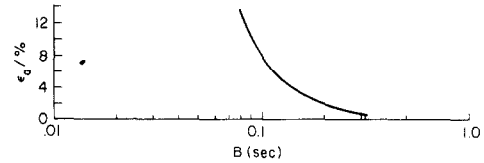

Fig. 10b. Variation of axial strain with viscoelasticity for Hanson's experiment 4-F.

The equations governing the wall and fluid motion are solved in conjunction with a measured stress–strain–strain-rate relation for the aorta obtained by Collins and Hu (1972a). Reasonable agreement with the experimental results of Hanson (1970) for decelerating dogs is shown for an appropriate value of the viscoelasticity parameter. However, the formulation and numerical solution by a Lax–Wendroff differencing scheme are sufficiently general to apply to a wide variety of materials and force fields with only minor modification. The numerical scheme has been found to be very stable when the stability criteria outlined above are adhered to. Periodic global checks on the fluid volume confirm its invariance to within 0·3 per cent throughout all calculations presented.

This study would indicate that aortic rupture may occur, when a subject is placed in a large decelerative or accelerative force field, by formation of a shock wave travelling along the aorta. The axial strains and

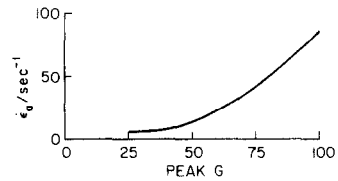

Fig. 11a. Variation of axial strain rate with peak acceleration for constant duration $T = 49{\cdot}5$ msec, $B = 0{\cdot}12$ sec.

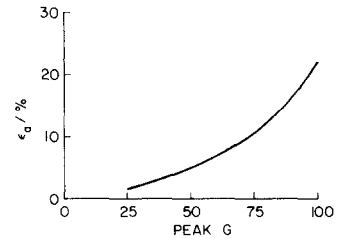

Fig. 11b. Variation of axial strain with peak acceleration for constant duration $T = 49{\cdot}5$ msec, $B = 0{\cdot}12$ sec.

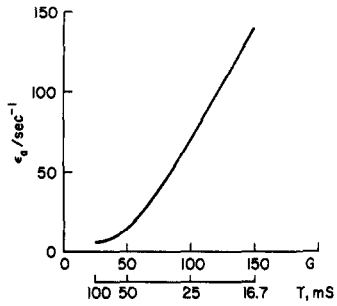

Fig. 12a. Variation of axial strain-rate with peak acceleration for constant $\int G dt$ = 15·7 m/sec, B = 0·12 sec.

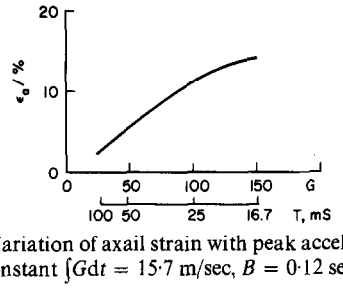

Fig. 12b. Variation of axail strain with peak acceleration for constant $\int G dt$ = 15·7 m/sec, B = 0·12 sec.

strain-rates of the aortic wall reach elevated values behind the shock front, and may well lead to stresses approaching the rupture level. All observed ruptures are transverse, accounting for an estimated 16 per cent (Greendyke, 1966) of all automobile fatalities in the United States.

In conjunction with better data on the ultimate rupture stress of the aorta, the present analysis will provide the levels of velocity and acceleration sufficient to produce such rupture. Tolerance levels so obtained will find direct application in the design of vehicles and passenger restraint systems for human safety.

It has become increasingly apparent through this investigation that the high sensitivity of strain and strain-rate to small variations in the parameters characterizing the viscoelasticity of the wall material may well afford a useful means of determining material properties by careful shock wave experiments.

Acknowledgements—The authors are indebted to P. G. Hanson, M.D. for furnishing them with original detailed records of his experimental measurements, and to I. I. Lasky, M.D. for drawing to our attention many interesting articles in the medical literature on this subject.

REFERENCES

Anliker, M., Rockwell, R. L. and Ogden, E. (1971) Nonlinear analysis of flow pulses and shock waves in arteries—I–II. *ZAMP* **22,** 217–246; 563–581.

Beck, C. S. (1935) Contusions of the heart. *J. Am. Med. Assoc.* **104**(2), 109–114.

Collins, R. and Hu, W. C. L. (1972a) Dynamic deformation experiments on aortic tissue. *J. Biomechanics* **5,** 333–337.

Collins, R., Lee, K. J., Lilly, G. P. and Westmann, R. A. (1972b) Mechanics of pressure cells. *Exper. Mech.* **12**(11), 514–519.

Fidler, H. K. (1949) Traumatic rupture of the thoracic aorta. *Canad. Med. Assoc. J.* **60,** 590–595.

Gable, W. D. and Townsend, F. M. (1963) An analysis of cardiovascular injuries resulting from accelerative force. *Aerospace Med.*, 929–934.

Greendyke, R. M. (1966) Traumatic rupture of the aorta. *J. Am. Med. Assoc.* **195,** 527–530.

Hanson, P. G. (1970) Pressure dynamics in thoracic aorta during linear deceleration. *J. appl. Physiol.* **28**(1), 23–27.

Kroell, C. K., Schneider, D. C. and Nahum, A. M. (1971) Impact tolerance and response of the human thorax. *Proc. 15th Stapp Conference.*

Lambert, J. W. (1958) On the nonlinearities of fluid flow in non-rigid tubes. *J. Franklin Inst.* **266,** 83.

Lundevall, J. (1964) The mechanism of traumatic rupture of the aorta. *Acta Path. Microbiol. Scand.* **62,** 34–46; (Also *Norsk Laegeforening Tidsskrift*, 440–444, March, 1963).

Macgregor, C. W. and Fisher, J. C. (1946) A velocity modified temperature for the plastic flow of metals. *J. appl. Mech.* **A,** 11–16.

McClintock, F. A. and Argon, A. S. (1966) *Mechanical Behavior of Materials.* Addison-Wesley, Mass.

McDonald, J. B. and Campbell, W. A. (1945) Traumatic rupture of the normal aorta in young adults. *Am. Heart J.* **30**(4), 321–324.

Olsen, J. H. and Shapiro, A. H. (1967) Large amplitude unsteady flow in liquid-filled elastic tubes. *J. Fluid Mech.* **29,** 513–538.

Patel J. W. *et al.* (1968) Traumatic rupture of the thoracic aorta. *J. Am. Med. Assoc.* **203** (12), 118–120.

Polmanteer, K. E., Servais, P. C. and Koinkle, G. M. (1952) Low temperature behavior of silicone and organic rubbers. *Ind. Engng Chem.* **44,** 1576–1581.

Richtmyer, R. D. and Morton, K. W. (1967) *Difference Methods for Initial Value Problems*, Sect. 12.7, 13.4. Interscience, New York.

Rindfleisch, E. (1893) Zur Entstehung und Heilung des An eurysma Dissecans Aortae. *Virch. Arch. Path. Anat.* **131,** 374–378.

Roberts, V. L. and Beckman, D. L. (1970) The mechanisms of chest injuries. In *Impact Injury and Crash Protection* (Edited by Gurdjian, E. S. *et al.*) Chap. 4. Charles C. Thomas, Illinois.

Rudinger, G. (1970) Shock waves in mathematical model of the aorta. *J. appl. Mech.* **37,** 34.

Rutherford, P. S. (1951) Traumatic rupture of aorta. *Br. Med. J.*, 1337.

Shennan, T. (1928) Traumatic (false) aneurysm of the aorta. *J. Path.* **32,** 795–798.

Smith, T. L. (1962) Nonlinear viscoelastic response of amorphous elastomers to constant strain rates. *Trans. Soc. Rheol.* **VI,** 61–80.

Strassman, G. (1947) Traumatic rupture of the aorta. *Am. Heart. J.* **33,** 508–515.

Taylor, E. R. (1962) Thrombocytopenia following abrupt deceleration, ARL-TDR-62-30, 6571*st* ARL, AMD, AFSC, Holloman AFB, New Mexico.